

A SOLAR WARMING MODEL (SWarm) TO ESTIMATE DIURNAL CHANGES IN NEAR-SURFACE SNOWPACK TEMPERATURES FOR BACK-COUNTRY AVALANCHE FORECASTING

Laura Bakermans^{1,*} and Bruce Jamieson^{1,2}

¹Department of Civil Engineering, ²Department of Geoscience, University of Calgary, Calgary, Canada

ABSTRACT: Diurnal temperature fluctuations occur in near-surface snowpack layers as a result of the energy balance at the snow surface. While there is some understanding of these temperature fluctuations and their effects on snowpack stability, quantified estimates of their magnitude are not readily available to avalanche forecasters in western Canada.

During the winters of 2005 and 2006, near-surface temperatures were measured on a knoll located in the Columbia Mountains of British Columbia. The field dataset was used to develop a near-surface warming model, based on linear regression analysis of predictor variables derived from surface energy flux terms. To facilitate use in large forecast areas where representative meteorological data are typically scarce, consideration was given to the availability of input data. Based on slope, aspect, expected cloud cover and number of days since snowfall, the model predicts the magnitude of near-surface daytime warming with an estimated root mean square error of 1.6 °C.

KEYWORDS: solar radiation, short wave radiation, near-surface warming, surface energy balance, snowpack temperatures, avalanche forecasting

1. INTRODUCTION

Daytime warming in the upper snowpack can have important effects with respect to skier-triggered avalanches. These include changes in the mechanical properties of slabs (e.g. McClung and Schweizer, 1997; McClung, 1996) and the creation of conditions favourable for the formation of weak snow layers (e.g. Birkeland, 1998). Although additional research is required to fully understand the relationship between near-surface warming and avalanches (e.g. Exner and Jamieson, 2008a), experienced avalanche practitioners usually consider near-surface warming, among many other factors, when evaluating snow instability.

This paper outlines the development of a model intended to provide avalanche practitioners in Canada with quantitative information about the expected magnitude and spatial variation of near-surface daytime warming. Like most other Class II (snowpack) and Class III (meteorological) factors, daytime warming will not be important in every instability evaluation.

1.1 Current observations

Currently, of the many observations typically considered during evaluation of snow

instability in Canada, snow temperature and solar (short wave) radiation are the two that relate best to near-surface warming. The temperature at 10 cm depth below the snow surface (T_{10}) is a standard study plot measurement outlined in the Canadian Avalanche Association *Observation Guidelines and Recording Standards for Weather, Snowpack and Avalanches* (CAA, 2002, p.4). Surface temperature and sub-surface temperatures at 10 cm increments are also standard measurements at profile sites (CAA, 2002, p. 15). While these data give some indication of near-surface snow temperatures, they are not typically taken at sufficient spatial and temporal resolution to identify daytime changes in near-surface temperature (i.e. warming), or to illustrate how near-surface temperatures vary over terrain. Radiometers can be used to measure incoming solar radiation, but they are not common due to cost and maintenance issues (McClung and Schaerer, 2006, p. 206). Instead qualitative assessments of cloud cover, surface melting and intensity of insolation (e.g. felt on bare skin) typically provide the only available information about solar radiation.

1.2 Physically based models

CROCUS (Brun et al., 1992) and SNOWPACK (Bartelt and Lehning, 2002) are two physically-based computer models that simulate the layered structure of the snowpack and

*Corresponding author address: Laura Bakermans, PO Box 5307, Smithers, BC, Canada, V0J 2N0; email: lbakermans@yahoo.ca

metamorphism of snow crystals once deposited. Because detailed surface energy balance calculations are undertaken in order to model these snowpack processes correctly, these models can provide quantitative information about near-surface warming. Because both models require high quality automated meteorological input data (including radiometer data), operational use is limited in North American avalanche forecasting programs.

Although some professional avalanche forecasting operations in Canada (e.g. highways control teams) have access to automated meteorological data, many (e.g. commercial guiding operations) rely primarily on extensive field observations. Based on the forecast areas for which the Canadian Avalanche Centre issues public bulletins and advisories, the extent of avalanche terrain in western Canada is greater than 300,000 km². Within this area, about 435 weather stations provide data potentially accessible to avalanche forecasting operations. It is estimated that less than 10% of these are automated weather stations located at or above treeline, and fewer than 2% include radiometers.

2. BACKGROUND

Near-surface warming occurs as a result of the energy balance at the snow surface. Mechanisms of energy exchange that contribute to the total surface energy flux, which is energy available to change temperature or phase at the snow surface, are given in Equation 1. An additional term is often included to account for energy added to the snowpack by precipitation. Energy fluxes into the snowpack are typically defined as positive.

$$Q_t = Q_{sw} + Q_{lw} + Q_s + Q_l + Q_c \quad (1)$$

where Q_t = total surface energy flux
 Q_{sw} = short wave radiation flux
 Q_{lw} = net long wave radiation flux
 Q_s = sensible turbulent (convective) heat flux
 Q_l = latent turbulent (convective) heat flux
 Q_c = conductive heat flux

Male and Gray (1981) and Obled and Harder (1978) both provide a detailed description of surface energy fluxes contributing to snowmelt and the factors that influence them. The relative importance of each term varies due to differences

in location, terrain, snowpack characteristics, meteorological conditions, day of year and time of day. Many discussions of the surface energy balance suggest that net radiation (short and long wave) is often the largest component (e.g. Obled and Harder, 1978; Male and Granger, 1981; Plüss, 1997).

3. FIELD METHODS

Field data were collected on Gopher Butte (51°14'17" N, 117°42'10" W, 1940 m), a treeline knoll near the Mount Fidelity research station and study plot (1905 m) in Glacier National Park (Figure 1). The field site is located within the Columbia Mountains of British Columbia, Canada, which Hägeli and McClung (2003) describe as having a transitional snow climate with a strong maritime influence.

For each of the eleven different measurement periods undertaken during the winters of 2005 and 2006, thermocouple arrays were set up at a flat location on the knoll top and at three undisturbed locations on the knoll side slopes to measure near-surface temperatures (Figure 2). For each measurement period, which ranged in length from one to six days, the side slope arrays were positioned on different aspects. To maintain measurement depths close to the snow surface, the field equipment was only set up during periods without forecast precipitation.

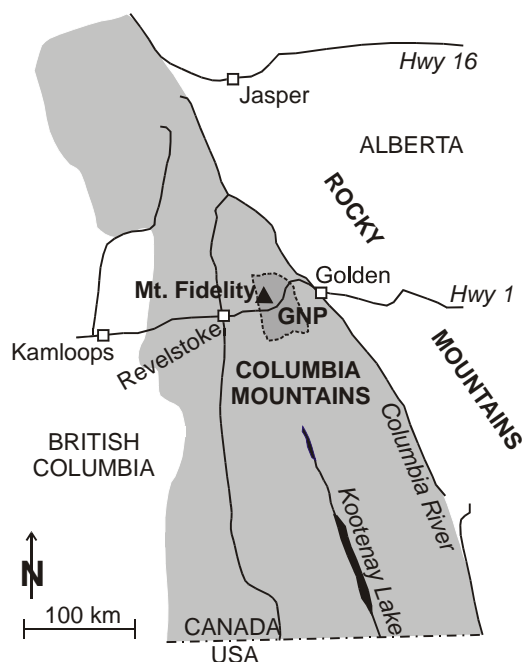


Figure 1: The location of the study site at Mount Fidelity in Glacier National Park (GNP).

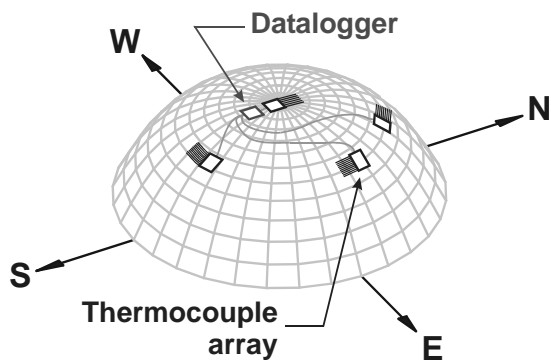


Figure 2: Typical array placement. Knoll slope arrays were placed on different aspects for each field experiment.

Each array consisted of ten chromel-alumel thermocouples placed at varying depths within the top 30 cm of the snowpack. Each thermocouple was glued to the underside of a balsa wood section to facilitate placement within the snowpack (Figure 3). The equipment was then painted with white acrylic spray paint in an attempt to mimic the highly reflective properties of snow. A Campbell Scientific Ltd. CR10X datalogger recorded average temperature values for each thermocouple, typically at a 15 minute interval.

The physical and optical properties of snow contribute to the difficulty in obtaining accurate measurements of near-surface temperature. Several studies that included field measurements of near-surface temperature report equipment-related differences between measured and expected values (e.g. Andreas, 1986; Brandt and Warren, 1993; Morstad, 2004). Despite steps taken to reduce differences between the properties of the measurement equipment and the

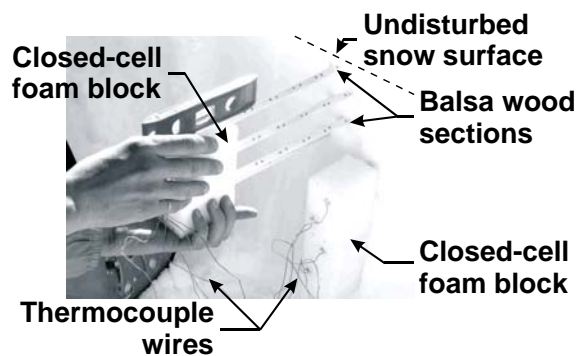


Figure 3: Equipment used in 2006 to collect field measurements of near-surface snow temperatures. Equipment was backfilled with snow prior to measurement.

snow, the field data included near-surface snow temperatures greater than zero degrees Celsius. Temperature data collected when near-surface snow conditions were isothermal, and during experiments in which arrays were shaded from direct short wave radiation for brief periods, helped to quantify these measurement errors. Estimates based on both types of data indicate that, under non-melt conditions, the magnitude of measurement errors at depths of 10 cm or greater were less than 0.3 °C (Bakermans, 2006, pp. 146-156). At 5 cm depth, the magnitude increased to approximately 1 °C.

Manual measurements of daytime air temperature and snow surface temperature at the array sites were made at approximately hourly intervals during each measurement period. Air temperature measurements were made with an Oakton Acorn Temp 5 thermometer, held approximately 1.5 m above the snow surface and shaded with a snow shovel blade. A Testo 825-T4 infrared thermometer, with adjustable emissivity set to 0.99, was used for the snow surface temperature measurements. Manual observations of sky condition, estimated wind speed and snow surface condition (i.e. sunny or shaded) were also recorded.

Automated meteorological data from the nearby Mount Fidelity study plot were available for analysis. These included air temperature, precipitation, relative humidity, incoming short wave radiation, incoming long wave radiation, wind speed and wind direction, all measured at hourly intervals. Radiation data were collected with an Eppley Precision Spectral Pyranometer and an Eppley Precision Infrared Radiometer. These instruments, mounted facing upwards, were continuously ventilated with AC power. During near-daily visits to the study plot, field staff manually removed any accumulated snow from the snow-shedding dome surrounding each sensor.

Manual snow profiles to a depth of approximately 40 cm were completed in undisturbed snow near each array site to obtain information about snowpack characteristics. Snow profiles were completed following the procedure outlined in the Canadian Avalanche Association Observation Guidelines and Recording Standards (CAA, 2002, pp. 13-19).

4. DATASET

Near-surface temperature changes in the upper portion of the snowpack were quantified by determining the magnitude of daytime warming at vertical depths of 10 and 15 cm below the snow surface. Daytime warming (ΔT_d) was defined as the difference, at vertical depth d , between the temperature at sunrise and the maximum afternoon temperature (Figure 4). Vertical depths were used in this analysis because they are consistent with the manual snow temperature measurement techniques used by avalanche practitioners in Canada (CAA, 2002, p. 15). In subsequent sections, d refers to vertical depth and z refers to the corresponding slope-normal distance from the snow surface.

Data collected at depths shallower than 10 cm were not included in the model building dataset because they were subject to substantial measurement errors, as previously discussed. Data collected at depths greater than 15 cm were also excluded because of the decrease in diurnal warming at these depths. The magnitude of ΔT_d , which decreased with depth below the snow surface, was usually less than 1 °C at the lower limit of the field measurements (approximately 30 cm depth).

For all measurement days with sufficient data, the temperature at sunrise and the afternoon peak temperature were interpolated linearly, at 10 and 15 cm vertical depths; ΔT_{10} and ΔT_{15} were then calculated. Prior to interpolation, field data

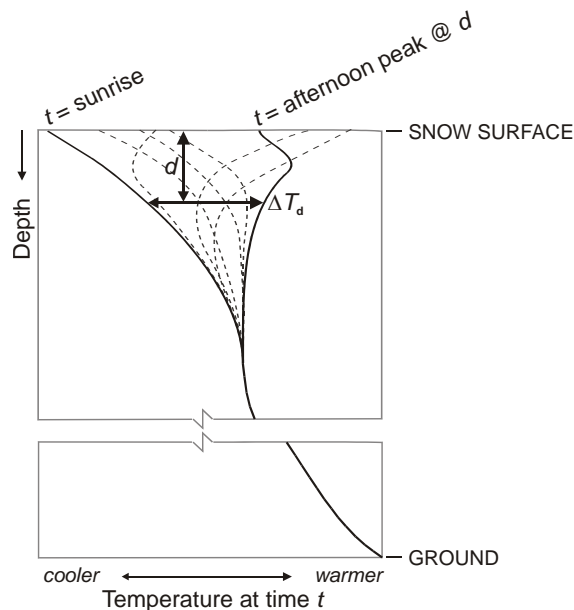


Figure 4: Daytime warming (ΔT_d) relative to temperature profiles at different times t .

were adjusted to reflect thermocouple-specific offsets measured during periodic calibration in a snow-water slurry. Any data for which the measured maximum afternoon temperature reached 0 °C were excluded. The final dataset consisted of 80 ΔT_d measurements collected in the months of February, March or April, under cloud cover conditions ranging from clear to overcast. Temperature measurements were not made on a directly west-facing slope due to tree cover on Gopher Butte, but the dataset included ΔT_d values measured on the knoll top and all other aspects.

It is important to recognize the limitations to this small dataset. The measured temperatures are representative of a treeline knoll in midwinter. Although some variation in upper snowpack conditions (e.g. hardness, density) is included in the dataset, there may be some conditions (e.g. thick near-surface crust) under which the subsequent variation in snow surface albedo, extinction of short wave radiation and/or conductivity may substantially influence daytime warming. All of the field data were collected on days with little wind or precipitation. The measured daytime warming values, therefore, do not reflect energy exchange at the snow surface resulting from precipitation or under conditions favourable for strong convective heat transfer.

5. ANALYSIS

Daytime warming (ΔT_d) was selected as the dependent variable for the model building analysis. Several potential predictor variables were then identified for each of the following surface energy balance terms: short wave radiation flux, net long wave radiation flux and convective heat flux (conduction was considered in combination with net long wave radiation flux and convective heat flux rather than as a separate term on its own). The potential predictor variables varied in complexity and, although we attempted to maintain a physical basis for each, availability of input data and ease of calculation were key considerations in their development. For a detailed description of the potential predictor variables included in the analysis, refer to Bakermans (2006, pp. 103-113). The use of slope normal distances below the snow surface rather than vertical depths to calculate potential predictor variables caused very slight differences between the results of this analysis and those reported in Bakermans (2006, chapter 6).

5.1 Correlation analysis

To determine which variables to include in a multivariate linear regression analysis, and to evaluate different methods of estimating snowpack parameters such as albedo, short wave radiation extinction coefficient and conductivity, correlation analysis against ΔT_d was undertaken. For each of the surface energy flux terms included in the analysis (i.e. short wave radiation flux, net long wave radiation flux and convective heat flux) Pearson and Spearman rank correlations both identified the same predictor variable as having the strongest relationship with ΔT_d .

5.2 Multivariate linear regression with measured incoming radiation variables

The predictor variables identified as having the strongest relationship with ΔT_d were incorporated in a backwards stepwise multivariate linear regression against ΔT_d . Due to the relatively small size of the dataset, no data were withheld from the regression analysis for subsequent model testing.

One assumption of multivariate linear regression is the independence of prediction errors. The rate of Type I errors (i.e. incorrect rejection of a null hypothesis) will increase if prediction errors are significantly autocorrelated, (Tabachnick and Fidell, 2001, pp. 121-122). Because the model building dataset includes ΔT_d measurements collected at the same depth on adjacent days and on the same day at adjacent depths, there is potential for autocorrelation of prediction errors. However, this effect is expected to be small because the dataset includes measurements made at different locations over eight different measurement periods.

Of the predictor variables included in the regression analysis, the only significant term ($p < 0.05$) identified was the following simplified approximation of short wave radiation at depth.

$$SW_{\max} \cdot (1-\alpha)/z$$

where SW_{\max} = daily maximum incoming short wave radiation value measured at the Mount Fidelity study plot, projected to the appropriate slope angle and aspect ($W \cdot m^{-2}$)

α = snow surface albedo

z = slope normal distance below the snow surface (m)

Snow surface albedo was estimated using the following parameterization obtained from Baker et al. (1990).

$$\alpha = 0.839 - 0.0473 \cdot N^{0.5} \quad (2)$$

where N = number of days since snowfall

Regression results are summarized in Table 1 for the entire dataset, and for the dataset with one statistically identified outlier removed. The criterion used for outlier identification was a residual value greater than three times the standard deviation of the residuals. The regression intercepts (B_0) are not included because, in both cases, they were small in magnitude and not significant.

We used both the Kolmogorov-Smirnov (K-S) and the Lilliefors tests for normality. The Lilliefors test adjusts the K-S p -value to account for estimation of the mean and standard deviation from the sample (Lilliefors, 1967). For the entire dataset, normality of the regression residuals is not rejected at $p = 0.05$ using the K-S test ($D = 0.129$, $p < 0.15$), but is rejected with the Lilliefors test ($p < 0.01$). With the statistically identified outlier removed, normality of the regression residuals is not rejected at $p = 0.05$ using the K-S test ($D = 0.112$, $p > 0.20$), but is again rejected with the Lilliefors test ($p < 0.05$).

Further analysis with six additional outliers (residual values greater than two times the standard deviation of the residuals) removed indicates that the regression coefficients are not sensitive to outliers in the dataset ($B = 0.00455$). With all seven outliers removed, normality of the regression residuals is not rejected with either the K-S ($D = 0.080$, $p > 0.20$) or Lilliefors ($p > 0.20$) tests.

Table 1: Results of backwards stepwise regression (presented for the complete dataset and for the dataset with one statistically identified outlier removed).

Predictor variable	n	Coefficient (B)	Std. error of B	p of B	Adj. r^2	p	Std. error of est. ($^{\circ}C$)
$SW_{\max} \cdot (1-\alpha)/z$	80	0.00450	0.000313	< 0.001	0.72	< 0.001	1.24
	79	0.00446	0.000290	< 0.001	0.75	< 0.001	1.15

5.3 Linear regression with estimated incoming short wave radiation

Because radiometer data is not available for most avalanche forecasting operations in western Canada, and in order to create a model that can be used as a predictive or learning tool, the regression analysis was repeated using a simple method of estimating the daily maximum incoming short wave radiation value. Equations 3 and 4, obtained from a review of short wave radiation parameterizations prepared by Niemelä et al. (2001), were selected from several calculation methods evaluated against data collected in the Mount Fidelity study plot. The original source of each equation is provided in italics below.

$$SW_{\text{clr}} = S_0 \cdot \cos\theta \cdot (0.47 + 0.47 \cdot \cos\theta) \quad (3)$$

Moritz, 1978

$$SW_{\text{all}} = [(1 - c) + t_c \cdot c] \cdot SW_{\text{clr}} \quad (4)$$

Berliand, 1960

where SW_{clr} = clear sky incoming short wave radiation ($W \cdot m^{-2}$)
 SW_{all} = all sky incoming short wave radiation ($W \cdot m^{-2}$)
 S_0 = solar constant ($1367 W \cdot m^{-2}$)
 θ = solar zenith angle
 c = cloudiness (decimal fraction)
 t_c = cloud transmissivity (assumed to be 0.48)

A significant ($p < 0.001$) coefficient of determination ($r^2 = 0.83$) was found between the values estimated with Equations 3 and 4 and measured values in a dataset ($n = 102$) consisting of all positive incoming short wave radiation measurements from the winters of 2005 and 2006 for which a corresponding manual sky observation was available (Bakermans, 2006, pp. 162-166). Cloudiness was estimated from the manual sky observations.

For each measurement day in the dataset, hourly incoming short wave radiation estimates were calculated from manual sky condition observations using Equations 3 and 4. After projecting the estimates to the appropriate slope and aspect (Walraven, 1978; Robinson, 1966,

chapter 2), a daily maximum value corresponding to each ΔT_d measurement was extracted (eSW_{max}).

Regression results for $eSW_{\text{max}} \cdot (1-\alpha)/z$ against ΔT_d are summarized in Table 2; no data with residuals greater than three times the standard deviation of the residuals were identified in this analysis. The regression intercept (B_0) is not included because it was not significant and had a standard error larger than the magnitude of B_0 . Normality of the regression residuals is not rejected at $p = 0.05$ using either the K-S test ($D = 0.095$, $p > 0.20$) or the Lilliefors test ($p < 0.10$).

5.4 Assessment of model performance

As neither a separate portion of the initial dataset nor additional independent data were available for model testing, cross validation was undertaken to obtain estimates of expected model errors (Wilks, 1995, pp. 194-195). The complete dataset ($n = 80$) was randomly divided into 10 folds of equal size. In turn, each fold was withheld while linear regression of ΔT_d on $SW_{\text{max}} \cdot (1-\alpha)/z$ was completed with the remaining 72 data points. Regression equations were then applied to the withheld data and root mean square error (RMSE) values calculated. The same 10 folds were also used for cross-validation of ΔT_d on $eSW_{\text{max}} \cdot (1-\alpha)/d$. Results suggest model errors of approximately 1.3 °C and 1.5 °C, based on measured and estimated daily maximum incoming short wave radiation values, respectively.

6. MODEL LIMITATIONS

It is important to address the model limitations which result from the limited scope of the model building dataset, and from the simplifications made to accommodate readily available input data.

Incoming short wave radiation was the only significant predictor variable identified during the backwards stepwise regression analysis. If radiation data are not available, modelled ΔT_d values are sensitive to the accuracy of the incoming short wave radiation estimate. The simple incoming short wave parameterization used during model development, which does not

Table 2: Results of linear regression of $eSW_{\text{max}} \cdot (1-\alpha)/z$ against ΔT_d (no statistically identified outliers were identified).

Predictor variable	n	Coefficient (B)	Std. error of B	p of B	Adj. r^2	p	Std. error of est. (°C)
$eSW_{\text{max}} \cdot (1-\alpha)/z$	80	0.00542	0.000451	< 0.001	0.64	< 0.001	1.41

account for cloud opacity, will result in underestimation of incoming short wave radiation on days with thin cloud. Substantial changes in cloud cover during the day will also affect model performance, as neither the magnitude nor timing of changes in cloud cover are captured by a daily average value. A RMSE of 1.6 °C was calculated when the model was applied using maximum daily incoming short wave radiation values estimated from a single daily average cloudiness value.

Potential predictor variables that incorporated snowpack dependent parameters (e.g. conductivity, short wave radiation extinction coefficient) were considered in the model building analysis (Bakermans, 2006, pp. 103-113). The fact that these parameters were not identified as significant predictor variables simplifies the model input requirements. The indication that snowpack characteristics did not have a strong influence ΔT_d in our dataset may result from the difficulty inherent in accurately estimating these parameters from commonly observed snowpack characteristics. Under some conditions not represented in the dataset, like the presence of a thick near-surface crust, the effects of snowpack dependent parameters may be critical. This is expected to be less of a concern in areas where consistent new snowfall results in less variation in near-surface snowpack parameters.

The total snowpack depth on Gopher Butte was at least 1.5 m during each of the measurement periods. Model results would not apply under thin snowpack conditions, specifically if the snowpack was so shallow that the snow surface albedo was affected by the albedo of the underlying ground surface (e.g. snowpack depth < approximately 30 cm).

Because the model does not consider the initial snow temperature at depth and has no way to distinguish between energy that contributes to melting rather than temperature change, results are not valid when isothermal (0 °C) conditions are encountered in the upper snowpack layers. From an avalanche forecasting perspective, however, assistance recognizing and quantifying variability in daytime warming is perhaps more valuable under non-melt conditions than when surface melting is apparent. In a survey conducted amongst 35 experienced avalanche practitioners, many of the warming-related avalanche incidents reported were associated with cold, dry near-surface layers (Exner and Jamieson, 2008b).

The model does not consider shading, reflection or re-radiation by tree cover or by nearby terrain features. Because the magnitude of incoming short wave radiation can be adjusted for

these effects, there is potential to account for them in simple models like this one.

7. MODEL APPLICATION

The regression model developed from estimated incoming short wave radiation values requires the following input parameters to estimate ΔT_d :

- latitude and longitude
- slope
- aspect
- date
- expected cloud cover
- # of days since new snowfall

These data are all readily available to avalanche forecasters in Canada. The simplicity of the regression model also means that specialized software is not required, a benefit both in accessibility and in user-friendliness.

The example shown in Figure 5, prepared using Microsoft Excel, provides the model output visually. For use in field notes, etc., the output can be simplified as follows:

SWarm N, S (dry) if C

where N = ΔT_{10} on 40° north aspect
S = ΔT_{10} on 40° south aspect
C = expected sky condition (data codes as per CAA, 2006, p. 2)

This format was used by the University of Calgary Applied Snow and Avalanche Research field staff as a standardized method of recording and communicating the daytime warming information estimated using the model. A Microsoft Excel version of the model (SWarm), similar to the example shown in Figure 5, is available for download from <http://www.schulich.ucalgary.ca/Civil/Avalanche/papers.htm>.

Tremper (2001, p. 99) suggests that most back-country recreationists don't realize that radiation has a stronger effect on snow temperature than air temperature does. SWarm can also be used as a teaching tool to initiate discussion regarding near-surface daytime warming and its potential effects on stability. Input values can easily be changed to demonstrate the effects of cloud cover and time of year on the magnitude and spatial variability of daytime warming. Potentially, this understanding of snowpack warming over terrain will couple with field experience to reduce the avalanche risk associated with solar radiation.

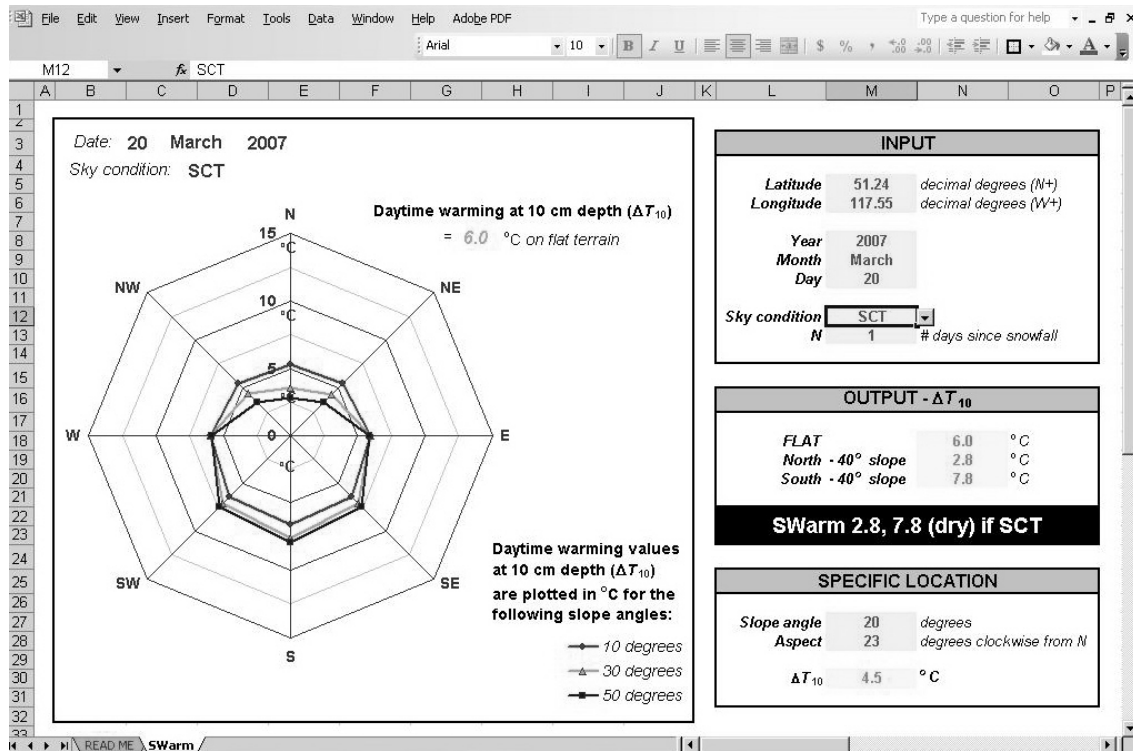


Figure 5: Model application example based on a Microsoft Excel spreadsheet.

8. SUMMARY

While incoming short wave radiation and near-surface daytime warming are recognized as factors having an effect on snowpack instability, quantitative information to include in the forecasting process is not readily available to most avalanche operations in western Canada. Correlation and linear regression analyses were undertaken to develop a semi-empirical warming model from field measurements of daytime warming.

Although many different parameters were included in the model building analysis, a variable based on daily maximum incoming short wave radiation proved to be the only significant predictor of near-surface daytime warming in this limited dataset. Based on hourly measurements of incoming short wave radiation, ΔT_0 was predicted with an expected RMSE of 1.3 °C. When incoming short wave radiation was estimated from daily average cloud cover, the RMSE increased to 1.6 °C.

A freely available spreadsheet-based model application (SWarm) was developed. In addition to providing a quantitative estimate of daytime warming to consider when evaluating snow instability, the model may also be useful as a teaching tool for less-experienced back-country travelers.

9. ACKNOWLEDGEMENTS

For their careful fieldwork, we are grateful to James Floyer, Dave Gauthier, Catherine Brown and Antonia Zeidler. Our thanks also to Charles Fierz with the Swiss Federal Institute for Snow and Avalanche Research and to the Avalanche Control Section of Glacier National Park, particularly Bruce McMahon and Jeff Goodrich, for a supportive field environment and practical insight. Jessica Smith with Campbell Scientific Canada, Joe Sabourin, Paul Lavoie and Rob Scorey from the University of Calgary Engineering Faculty Machine Shop and University of Calgary Civil Engineering Technologists Don Anson and Don McCullough all provided invaluable assistance with field equipment. Radiometer data were collected using instruments kindly loaned by The University of British Columbia Avalanche Research Group. We are grateful to Alliance Pipeline for their financial support of the Naomi Heffler Memorial Scholarship in Avalanche or Snow Science.

For support we are also grateful to HeliCat Canada, Canadian Avalanche Association, Mike Wiegeler Helicopter Skiing, Canada West Ski Areas Association and the Natural Sciences and Engineering Research Council of Canada.

10. REFERENCES

- Andreas, E.L. 1986. A new method of measuring the snow-surface temperature. *Cold Reg. Sci. Technol.*, 12, 139-156.
- Baker, D.G., D.L. Ruschy, and B.B. Wall. 1990. The albedo decay of prairie snows. *J. Appl. Meteorol.*, 29, 179-187.
- Bakermans, L. 2006. Near-surface snow temperature changes over terrain. (MSc thesis, University of Calgary.)
- Bartelt, P., and M. Lehning. 2002. A physical SNOWPACK model for the Swiss avalanche warning. Part I: Numerical model. *Cold Reg. Sci. Technol.*, 35, 123-145.
- Berliand, T.C. 1960. Method of climatological estimation of global radiation. *Meteorol. Gidrol.*, 6, 9-12. (Not seen; cited in Niemelä et al., 2001.)
- Birkeland, K.W. 1998. Terminology and predominant processes associated with the formation of weak layers of near-surface faceted crystals in the mountain snowpack. *Arctic Alpine Res.*, 30(2), 193-199.
- Brandt, R.E., and S.G. Warren. 1993. Solar-heating rates and temperature profiles in Antarctic snow and ice. *J. Glaciol.*, 39(131), 99-110.
- Brun, E., P. David, M. Sudul and G. Brunot. 1992. A numerical model to simulate snow-cover stratigraphy for operational avalanche forecasting. *J. Glaciol.*, 38(128), 13-22.
- Canadian Avalanche Association (CAA). 2002. *Observation guidelines and recording standards for weather, snowpack and avalanches*. Revelstoke, Canadian Avalanche Association.
- Exner, T. and B. Jamieson. 2008a. The effect of snowpack warming on the stress bulb below a skier. *Proceedings ISSW 2008, International Snow Science Workshop, Whistler, BC, Canada, 21-27 September 2008*, in press (this volume).
- Exner, T. and B. Jamieson. 2008b. Can solar warming contribute to dry slab avalanches? *Avalanche.ca - The Journal of the Canadian Avalanche Community*, Canadian Avalanche Association, Revelstoke, BC, 70-73.
- Hägeli, P., and D. McClung. 2003. Avalanche characteristics of a transitional snow climate - Columbia Mountains, British Columbia, Canada. *Cold Reg. Sci. Technol.*, 31, 255-276.
- Lilliefors, H.W. 1967. On the Kolmogorov-Smirnov test for normality with mean and variance unknown. *J. Am. Stat. Assoc.*, 62(318), 399-402.
- Male, D.H., and R.J. Granger. 1981. Snow surface energy exchange. *Water Resour. Res.*, 17(3), 609-627.
- Male, D.H., and D.H. Gray. 1981. Snowcover ablation and runoff. Chapter 9 in *Handbook of Snow*, Gray, D.M., and D.H. Male (eds.). Toronto, Pergamon Press.
- McClung, D.M. 1996. Effects of temperature on fracture in dry slab avalanche release. *J. Geophys. Res.*, 101(B10) 21,907-21,920.
- McClung, D., and P. Schaerer. 2006. *The Avalanche Handbook. 3rd Edition*. Seattle, The Mountaineers.
- McClung, D.M., and J. Schweizer. 1997. Effect of snow temperature on skier triggering of dry snow slab avalanches. *Proceedings of the International Snow Science Workshop, Banff, Alberta, Canada, 6-10 October 1996*, 113-117.
- Moritz, R.E. 1978. A model for estimating global solar radiation. Energy budget studies in relation to fast-ice breakup processes in Davis Strait. *Occasional Paper 26, Institute of Arctic and Alpine Research, University of Colorado, Boulder, Colorado, USA*, 121-142. (Not seen; cited in Niemelä et al., 2001.)
- Morstad, B.W. 2004. Analytical and experimental study of radiation-recrystallized near-surface facets in snow. (MSc thesis, Montana State University.)
- Niemelä, S., P. Räisänen and H. Savijärvi. 2001. Comparison of surface radiative flux parameterizations Part II. Shortwave radiation. *Atmos. Res.*, 58, 141-154.
- Obleed, C., and H. Harder. 1978. A review of snow melt in the mountain environment. *Proceedings, Modeling of Snow Cover Runoff* (S.C. Colbeck and M. Ray, editors). Hanover, New Hampshire: U.S. Army Cold Regions Research and Engineering Laboratory, 179-204.
- Plüss, C. 1997. The energy balance over an alpine snowcover: point measurements and areal distribution. *Zurcher Geographische Schriften*, 65, Verlag Geographisches Institut ETH, Zurich, Switzerland.
- Robinson, N. 1966. *Solar radiation*. New York, NY: American Elsevier Publishing Company.
- Tabachnick, B.G. and L.S. Fidell. 2001. *Using Multivariate Statistics*. Toronto, Allyn and Bacon.
- Tremper, B. 2001. *Staying Alive in Avalanche Terrain*. Seattle, WA: The Mountaineers Books.
- Walraven, R. 1978. Calculating the position of the sun. *Sol. Energy*, 20, 393-397.
- Wilks, D.S. 1995. *Statistical Methods in the Atmospheric Sciences*. San Diego, Academic Press.